

Fabrication and Characterization of Hierarchical Porous TiO₂ Films

YANHUA LI^{1,2,*} and DONGMING ZENG¹

¹College of Chemistry and Chemical Engineering, Central South University, Changsha 410083, P.R. China

²Department of Chemical Engineering and Information Engineering, Changsha Aeronautical Vocational and Technical College, Changsha 410019, P.R. China

*Corresponding author: Fax: +86 731 8830827; Tel: +86 731 8830827; E-mail: liyanhua12@yahoo.com.cn

(Received: 26 August 2011;

Accepted: 12 May 2012)

AJC-11470

Hierarchical porous TiO₂ films with macroporous and mesoporous structures are prepared by drop-coating a mixed solution of polystyrene spheres and TiO₂ colloid, followed by sintering to remove polystyrene spheres. XRD shows that crystal phase of TiO₂ particles is major anatase structure with minor brookite structure. AFM displays that particle size distribution of porous TiO₂ films ranges from 20-30 nm. SEM shows that TiO₂ films prepared by drop-coating TiO₂ colloid present mesoporous structure with a size of 8-50 nm. However, TiO₂ films prepared by drop-coating the mixture containing polystyrene spheres and TiO₂ colloid possess hierarchical porous structure with a mesoporous size of 8-50 nm and a macroporous size of about 600 nm. Besides, macropore ratios increase with increase of the ratio of polystyrene spheres to TiO₂ colloid. UV-visible absorption spectra indicate that porous TiO₂ films prepared at a polystyrene spheres/TiO₂ colloid ratio 1, have the highest absorption intensity.

Key Words: Porous TiO₂, Dye-sensitized solar cells, Fabrication, Characterization.

INTRODUCTION

There is currently a great deal of interest in synthesis of TiO₂ because of its important role in various applications, such as photo-catalysis¹, dye-sensitized solar cells^{2,3}, environmental purification⁴, gas sensors⁵ and electrochemical capacitors⁶. TiO₂ can be obtained by a wide range of synthetic methods, including but not limited to sol-gel method⁷, hydrothermal method⁸, precipitation⁹ and electrodeposition^{10,11}. Of these synthetic methods of TiO₂, sol-gel method is a most commonly applied method to make nanocrystalline TiO₂, however, nanoparticles made are amorphous in nature and require further heat treatment to obtain crystalline product¹². Hydrothermal method is one of the most widely used methods for increasing the crystallinity of TiO₂ and can be used to change crystal structure, morphology and phase composition of materials under the different reaction conditions¹³.

It is known that photo-catalytic activity of TiO₂ is strongly related to crystal structure, morphology, particle size, surface area and porosity¹². Furthermore, the phase and the degree of crystallinity of TiO₂ particles have great influence on specific applications¹⁴. TiO₂ nanoparticles are widely used in environmental purification owe to the high chemical inter, stability and high photo-catalytic activity^{15,16}. Porous nanocrystalline TiO₂ are used in dye-sensitized solar cells (DSSCs) because

of their high-energy conversion efficiency, simple preparation technology and low production costs^{2,17}. Morphology and microstructure of porous nanocrystalline TiO₂, including particle size, surface area and porosity, play an important role in energy conversion efficiency of dye-sensitized solar cells. There are many reports on porous TiO₂ widely used in dye-sensitized solar cells. However, these researches are only limited to mesoporous TiO₂ and hardly relate to hierarchical porous TiO₂ containing macroporous and mesoporous structures. Thus, it is necessary to study characterization of macroporous and mesoporous TiO₂.

In the present work, hierarchical porous films with macroporous and mesoporous structures were prepared by drop-coating the mixture containing polystyrene spheres and TiO₂ colloid with different ratios, followed by sintering to remove polystyrene spheres. Besides, UV-visible absorption spectra of dye adsorbed onto porous nanocrystalline TiO₂ films were studied. Thus far, there are several reports about syntheses of TiO₂ or TiO₂ composites by polystyrene spheres¹⁸. For example, Pei *et al.*¹⁸ fabricated hollow TiO₂ capsules through aging dissolution technique to remove the templates of core-shell composite spheres. However, hierarchical porous TiO₂ weren't prepared in their worker. The present paper aims to synthesize hierarchical porous TiO₂ with macroporous and mesoporous structures and study absorbance of UV-visible.

EXPERIMENTAL

All reagents were analytically pure and used without further purification. 600 nm polystyrene spheres were obtained from Interfacial Dynamics Inc. Phthalocyanine, isopropanol and tetrabutyl titanate were purchased from Sinopharm Chemical Reagent Ltd. Com., China. All of the solutions were prepared with deionized water purified by a Millipore Milli-Q Plus 185 purification system.

Laser particle size analyzer was used to monitor the size of TiO₂ colloid (Malvern, Mastersizer 2000). X-Ray diffraction (XRD) pattern was recorded on a Rigaku D/max 2500 with monochromatized CuK_α ($\lambda = 1.54056 \text{ \AA}$) incident radiation. Atomic force microscopy (PicoPlus, Agilent Technologies, CA, USA) was used to study the image of porous TiO₂. The size distribution and morphology of porous TiO₂ films were observed by scanning electron microscopy (FEI, Sirion200). An UV-3802 spectrophotometer was employed to record UV-Visible absorption spectroscopy of the samples.

General procedure

Preparation of TiO₂ colloid: 1 mL concentrated HNO₃ was added to a large conical flask with 150 mL water. Then, a mixture containing isopropanol and tetrabutyl titanate was dropwise added into the above solution under vigorous stirring at room temperature. The conical flask without being covered was put in a water bath. The reaction was carried out at 80 °C for 8 h under vigorous stirring and colloid was prepared. The above colloid was poured into a Teflon-lined autoclave and placed in the oven at 200 °C for 12 h. Finally, colloid treated by the autoclave was poured in beaker, redispersed by sonicating and concentrated to 10-11 %.

Preparation of porous TiO₂ films: TiO₂ colloid was mixed with polystyrene spheres with different ratios (polystyrene spheres/TiO₂ colloid = 0, 1:1, 2:1, 3:1). Two pieces of scotch tape were stuck on ITO as spacers to control the thickness of the film and the mixture containing polystyrene spheres and TiO₂ colloid was then coated in the space between the pieces of scotch tape. After rolled off the excessive mixture by a glass rod and dried, polystyrene spheres were then removed by sintering at 450 °C for 0.5 h. As a result, porous TiO₂ films were prepared.

Dye absorption on porous TiO₂ films: Porous TiO₂ films were immersed for 5 h in an ethanol solution of phthalocyanine in dark conditions at room temperature. Then, property of UV-Visible absorption spectroscopy of the dye absorption on the porous TiO₂ films was detected.

RESULTS AND DISCUSSION

Particle size of TiO₂ colloid: Particle size distribution of TiO₂ colloid was observed by laser particle size analyzer. Fig. 1 shows that the average particle size of TiO₂ colloid is about 92 nm and colloid particle size distribution ranges from 50-200 nm. Fig. 2 is particle size distribution of TiO₂ colloid in Fig. 1 according to different segment. It can be seen from the data in Fig. 2 that particle size of TiO₂ colloid below 67, 92 and 130 nm account for 10, 50 and 90 %, respectively.

XRD analyses of porous TiO₂ powder: Fig. 3 displays the XRD pattern of porous TiO₂ powder obtained by sintering TiO₂ colloid at 450 °C for 0.5 h. The XRD pattern can be

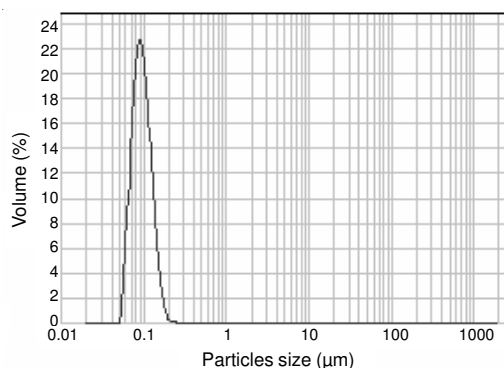


Fig. 1. Particle size distribution of TiO₂ colloid

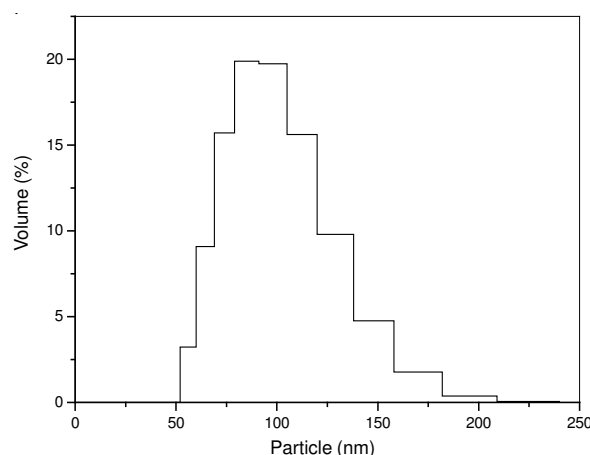


Fig. 2. Particle size distribution of TiO₂ colloid in the Fig. 1 according to different segment

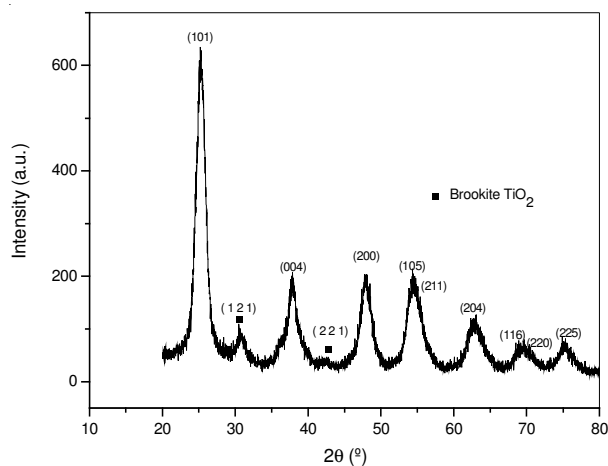


Fig. 3. XRD patterns of porous TiO₂ powder obtained by sintering TiO₂ colloid at 450 °C for 0.5 h

indexed to (101), (004), (200), (105), (211), (204), (116), (220) and (225) planes of tetragonal phase anatase TiO₂. All the peaks in the pattern are assigned to the fact that the porous TiO₂ particles formed are a mixture of largely anatase phase and minor brookite phase. With respect to the anatase phase mixed with the brookite phase, this is because there are the (121, 221) diffraction peaks of brookite phase and the (120) diffraction peak of brookite phase overlaps the (101) diffraction peak of anatase phase at $2\theta = 25.3^\circ$. Crystallite size is estimated from Scherrer formula¹⁹. Crystallite size of porous TiO₂ calculated through above Scherrer formula is 26 nm.

AFM of porous TiO₂ films: AFM image of porous TiO₂ films obtained with a polystyrene spheres/TiO₂ colloid ratio of 0 are showed in Fig. 4. AFM image shows that the morphology of porous TiO₂ films consists of spherical-like particles with a size of 20-30 nm, which is agreement with those detected by XRD. Particle size of TiO₂ colloid detected by laser particle size analyzer is larger than those of porous TiO₂ detected by AFM and XRD. The above behaviour can be explained as follows: laser particle size analyzer estimates the size of aggregated particles in the suspension, whereas techniques such as AFM and XRD estimate the size of the primary particles that make up the aggregate.

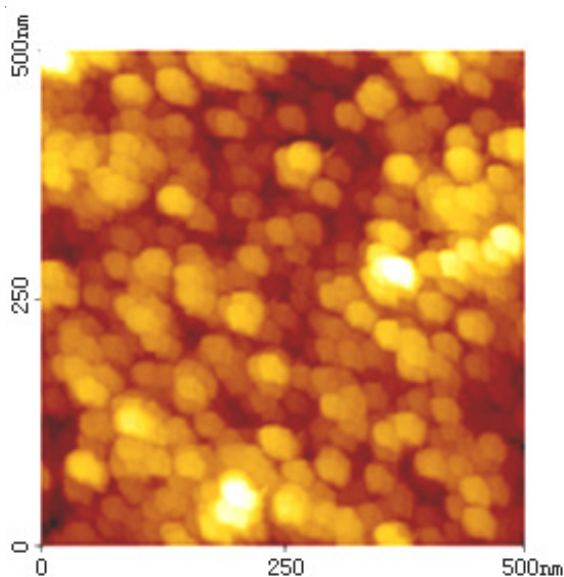


Fig. 4. AFM image of porous TiO₂ films obtained with a polystyrene spheres/TiO₂ colloid ratio of 0, followed by sintering TiO₂ colloid at 450 °C for 0.5 h

SEM of porous TiO₂ films: Fig. 5 illustrates SEM images of porous TiO₂ films prepared with a polystyrene spheres/TiO₂ colloid ratio of 0 (Fig. 5 a), 1:1 (Fig. 5b), 2:1 (Fig. 5 c) and 3:1 (Fig. 5d). As shown in Fig. 5a, the morphology of TiO₂ particles consists of spherical-like particles with a size of 8-30 nm and displays highly porous structure with a mesoporous size of 8-50 nm. However, except for porous structure with a mesoporous size of 8-50 nm, porous structure with a macroporous size of about 600 nm is observed in Fig. 5b-d due to removal of polystyrene spheres during sintering a mixture containing polystyrene spheres and TiO₂. In other words, hierarchical porous TiO₂ with macroporous and mesoporous structures is displayed in Fig. 5b-d. In addition, Fig. 5b-d also indicate that the ratio of macropore to mesopore increases with increase of the ratio of polystyrene spheres to TiO₂ colloid.

UV-Visible absorption spectra: Fig. 6 indicates UV-visible absorption spectra of phthalocyanine adsorbed onto porous TiO₂ films prepared with a polystyrene spheres/TiO₂ colloid ratio of = 0 (curve 1), 1:1 (curve 2), 2:1 (curve 3) and 3:1 (curve 4). There are two absorption peaks in all curves. In curves 1 and 4, the absorption peaks are exhibited at 411 and 586 nm. Absorption peaks exhibited 406 and 586 nm are shown in curve 2. Absorption peaks exhibited 408 and 586 nm are shown in curve 3. Besides, it can be observed that curve 2 (porous

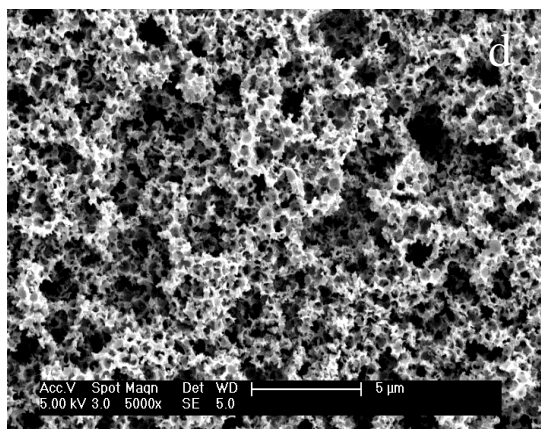
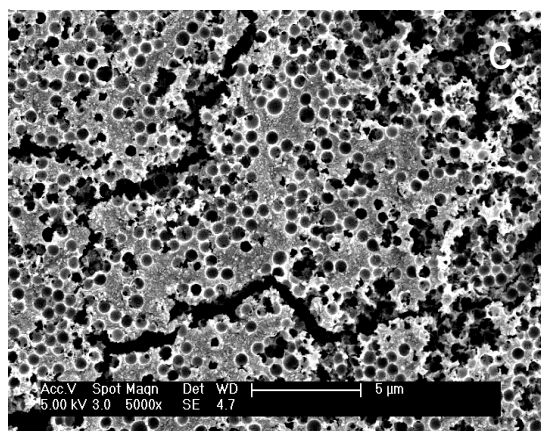
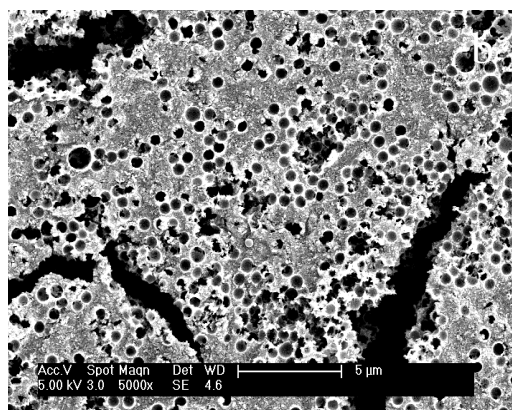
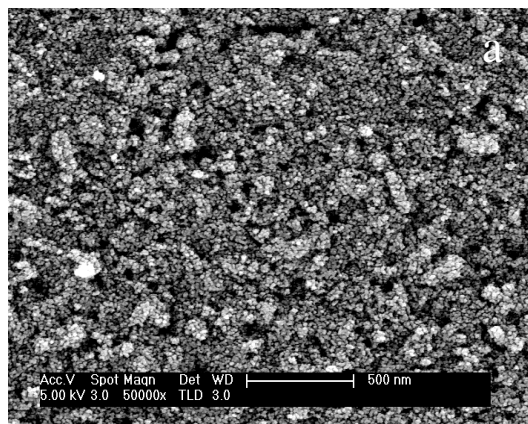


Fig. 5. SEM images of porous TiO₂ films prepared with a polystyrene spheres/TiO₂ ratio of 0 (a), 1:1 (b), 2:1 (c) and 3:1 (d), followed by sintering TiO₂ colloid at 450 °C for 0.5 h

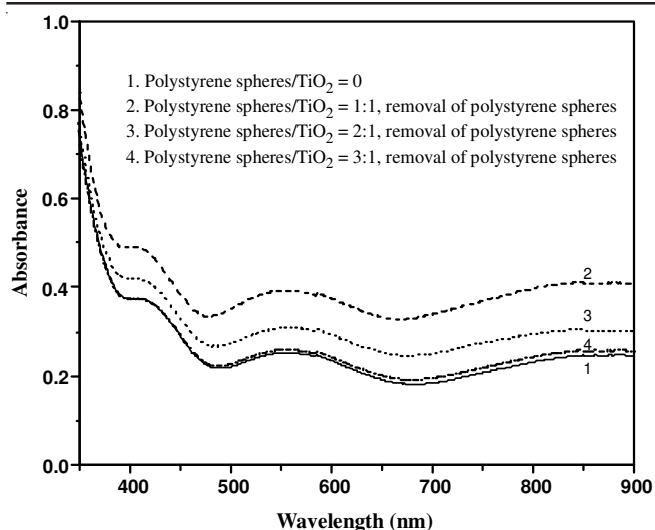


Fig. 6. UV-Visible absorption spectra of phthalocyanine adsorbed onto porous TiO₂ films

TiO₂ films prepared with a polystyrene spheres/TiO₂ colloid = 1:1) has the largest absorbance in all curves. Absorbance of curve 3 is inferior to that of curve 2, but superior to curves 1 and 4. It illustrates that porous TiO₂ films with the different ratio of macropore to mesopore have different UV-visible absorption intensity. The largest absorbance observed in curve 2 is possible attributed to the following interpretation: (1) porous TiO₂ have the optimum ratio of mesopore to macropore when they are prepared at a polystyrene spheres/TiO₂ colloid ratio of 1, since the size of the macropores (*ca.* 600 nm) is similar to the wavelength of the incident radiation (350-900 nm); (2) adsorption process itself in the porous TiO₂ films prepared at a polystyrene spheres/TiO₂ colloid ratio of 1 has the highest concentrations of dye and thus affects the intensities of the measured spectra. Shape and size have a significant impact on the optical and electronic properties of nanoparticles²⁰. It implies that porous TiO₂ prepared at a polystyrene spheres/TiO₂ colloid ratio 1 will possible have the highest energy conversion efficiency when they are used in dye-sensitized solar cells.

Conclusion

Hierarchical porous TiO₂ films with macroporous and mesoporous structures are successfully prepared. The result shows that crystal phase of TiO₂ are major anatase with minor brookite. Particle size distribution of porous TiO₂ films ranges from 20-30 nm. Porous TiO₂ films prepared by TiO₂ colloid present highly porous structure with a mesoporous size of 8-50 nm, whereas porous TiO₂ films prepared by using the

mixture containing polystyrene spheres and TiO₂ colloid possess highly porous structure with a meso-macroporous size of 8-50 and 600 nm, macropore ratios increase with increase of the ratio of polystyrene spheres to TiO₂ colloid. UV-Visible absorption spectra indicate that porous TiO₂ films prepared at a polystyrene spheres/TiO₂ colloid ratio of 1 have the highest absorption intensity. It implies that porous TiO₂ films prepared at a polystyrene spheres/TiO₂ colloid ratio 1 will possible have the highest energy conversion efficiency when they are used in dye-sensitized solar cells.

ACKNOWLEDGEMENTS

This work is supported financially by National Natural Science Foundation of China (No. 50972165) and Scientific Research Fund of Hunan Provincial Education Department (No. 09C1055).

REFERENCES

1. S.N. Hosseini, S.M. Borghei, M. Vossoughi and N. Taghavinia, *Appl. Catal. B*, **74**, 53 (2007).
2. B. O'Regan and M. Grätzel, *Nature*, **353**, 737 (1991).
3. W. Chen, X. Sun, Q. Cai, D. Weng and H. Li, *Electrochem. Commun.*, **9**, 382 (2007).
4. S. Ikezawa, H. Homyara, T. Kubota, R. Suzuki, S. Koh, F. Mutuga, T. Yoshioka, A. Nishiwaki, Y. Ninomiya, M. Takahashi, K. Baba, K. Kida, T. Hara and T. Famakinwa, *Thin Solid Films*, **386**, 173 (2001).
5. L.R. Skubal, N.K. Meshkov and M.C. Vogt, *J. Photochem. Photobiol. A*, **148**, 103 (2002).
6. T. Brezesinski, J. Wang, J. Polleux, B. Dunn and S.H. Tolbert, *J. Am. Chem. Soc.*, **131**, 1802 (2009).
7. M. Vishwas, S.K. Sharma, K.N. Rao, S. Mohan, K.V.A. Gowda and R.P.S. Chakradhar, *Spectrochim. Acta A*, **75**, 1073 (2010).
8. Y.M. Cui, L. Liu, B. Li, X.F. Zhou and N.P. Xu, *J. Phys. Chem. C*, **114**, 2434 (2010).
9. J.H. Lee and Y.S. Yang, *Mater. Chem. Phys.*, **93**, 237 (2005).
10. S. Karuppuchany, D.P. Amalnerkar, K. Yamaguchi, T. Yoshida, T. Sugiura and H. Minoura, *Chem. Lett.*, **30**, 78 (2001).
11. Y. Ishikawa and Y. Matsumoto, *Solid State Ionics*, **151**, 213 (2002).
12. A.R. Rao and V. Dutta, *Sol. Energy Mater. Sol. Cells*, **91**, 1075 (2007).
13. D.S. Kim and S.Y. Kwak, *Appl. Catal. A*, **323**, 110 (2007).
14. K.S. Yoo, T.G. Lee and J. Kim, *Micropor. Mesopor. Mater.*, **84**, 211 (2005).
15. H. Xu, X. Liu, M. Li, Z. Chen, D. Cui, M. Jiang, X. Meng, L. Yu and C. Wang, *Mater. Lett.*, **59**, 1962 (2005).
16. B. Su, Z. Ma, S. Min, S. She and Z. Wang, *Mater. Sci. Eng. A*, **458**, 44 (2007).
17. J.H. Kim, M.S. Kang, Y.J. Kim, J. Won, N.G. Park and Y.S. Kang, *Chem. Commun.*, 1662 (2004).
18. A.H. Pei, Z.W. Shen and G.S. Yang, *Mater. Lett.*, **61**, 2757 (2007).
19. B.R. Sankapal, M.C. Lux-Steiner and A. Ennaoui, *Appl. Surf. Sci.*, **239**, 165 (2005).
20. D.L. Liao and B.Q. Liao, *J. Photochem. Photobiol. A*, **187**, 363 (2007).